ON THE FEASIBILITY TO INVESTIGATE POINT DEFECTS BY ADVANCED ELECTRON MICROSCOPY

C. KISIELOWSKI, J.R.JINSCHEK
National Center for Electron Microscopy, Lawrence Berkeley National Laboratory, One Cyclotron Road 72-150, Berkeley, CA 94720, USA
E-mail: CFKisielowski.lbl.gov

Transmission Electron Microscopy evolves rapidly as a primary tool to investigate nano structures on a truly atomic level. Its resolution reaches into the sub Ångstrom region by now. Together with a better correction of lens aberrations, sensitivities are drastically enhanced. Utilizing advanced electron microscopes, it is feasible to promote experiments that aim to detect single atoms. This enables local investigations of non-stoichiometry. This paper reviews the current state-of-the–art.

1. Introduction

Traditionally, High Resolution Transmission Electron Microscopy (HRTEM) investigates the atomic structure of solids. The recorded lattice images can be related to structural models through image simulations. Over the last years, rapid technological progress including the manufacturing of field emission electron sources [1] and aberration correctors [2,3] led to the development of a novel microscope generation [4,5,6]. Already the current microscope generation images the crystal structure directly [7,8], enables spectroscopy on a single atom column [9], and extends resolution to sub Ångstrom values [5,8,10]. Combined with suitable equipment for in-situ experimentation, real time TEM observations progress rapidly. For example, a quantized resistance in gold nanowires was reported while imaging a single chain of gold atoms [11]. Other examples for in-situ experimentation are highlighted in these proceedings [12].
In this development it is of equal importance that sensitivities were drastically improved. Most noticeable are recent reports about the detection of light elements, single atoms, impurities, and vacancy segregation [5,8,13,14,15]. These are typical aspects related to the local stoichiometry of materials. The paper reviews these developments and provides guidelines for single atom detection of elements from the Periodic Table by the two most common imaging techniques. Further, it is pointed out that the preparation of electron transparent samples becomes more demanding since tighter boundary conditions related to sample surface roughness must be met in experiments aiming for point defect visualization.
Relevant features of HRTEM will be outlined in the second section of the paper together with a treatment of the High Angle Annular Dark Field (HAADF) method that is commonly referred to as “Z-contrast microscopy”. Section three compares both experiments, gives examples, and concludes the paper.

2. Phase contrast - and Z contrast microscopy

Figure 1 depicts the principle of HRTEM- and HAADF imaging. HRTEM is a single shot technique that utilizes coherently scattered electrons that form lattice images recorded on film or CCD cameras. Traditionally, image simulations are necessary to relate the recorded beam interferrograms to the crystal structure since defocus, other lens aberrations, and sample thickness change the image patterns rapidly. Recent progress with image processing, however, allows for recovering the complex electron exit wave (EWR) from a focal series of lattice images [16,17]. In this holographic reconstruction process the defocus dependence is eliminated and lens aberrations can largely be reduced. Such reconstructed images depict the projected crystal structure directly if the samples are thin (<10 nm). Further, the procedure extends the resolution of microscopes to their information limit that can reach sub Ångstrom values.

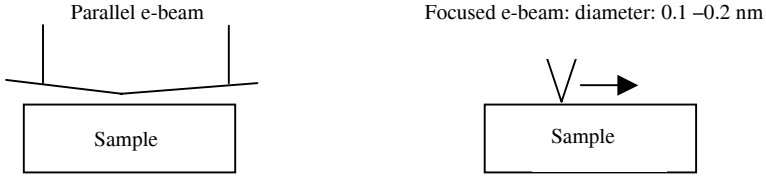

Fig. 1) Left: HRTEM utilizes a parallel incident beam that is scattered in the sample and recorded on a CCD camera (film). The lattice images are interferrograms of coherently scattered beams. Right: In HAADF imaging, the sample is illuminated with a convergent electron beam of 0.1-0.2 nm of diameter on the sample that is scanned to form an image. A HAADF ring detector is used to collect incoherently scattered electrons.

In HAADF imaging the electron beam is scanned and incoherently scattered electrons are recorded which is why it produces direct crystal images without additional processing. The images are very similar to reconstructed phase images except for a smaller signal to noise ratio as shown in Figure 2. They depict the 1s state of the electron wave trapped in the Coulomb Potential of the atomic columns [18,19]. There are, however, distinct and important differences concerning the thickness dependence of the signals and the chemical discrimination between atoms of different atomic number Z that will be addressed next.

Figure 3 shows calculations that describe the local image intensity in phase - and Z contrast images as a function of sample thickness. An artificial fcc crystal structure is considered where the lattice sites are occupied with the different elements carbon (Z=6), aluminum (Z=13), gallium (Z=31), indium (Z=49), and gold (Z=79). Multi-slice calculations were employed [22] to calculate the zero beam intensity that characterizes the behavior of phase contrast signals with sample thickness. We assumed thin crystals and a Rutherford scattering process

to calculate the image intensity as a function of sample thickness in Z contrast images [13].

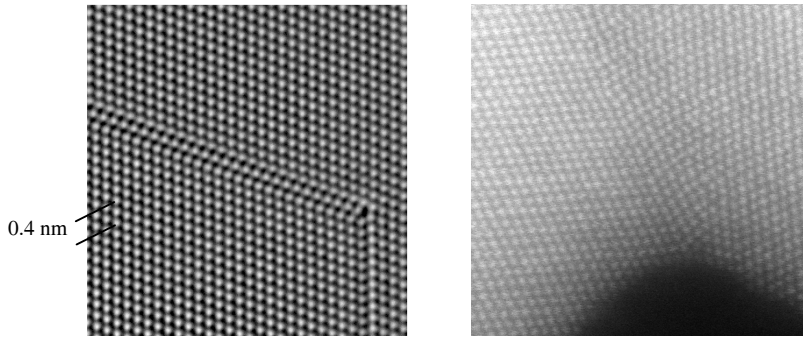

Figure 2: Left: Phase of the electron exit wave reconstructed from 20 lattice images of a dislocation in gold [110]. Right: HAADF image of a grain boundary in gold [110][20.21].

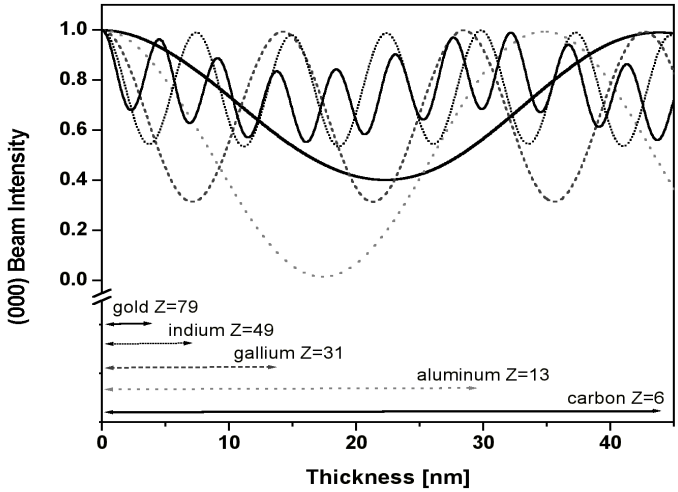

Figure 3: Zero beam intensity versus sample thickness of a fcc crystal with lattice parameter a=0.4 nm and lattice sites occupied by the indicated elements.

It is seen from Figure 3 that phase contrast signals oscillate with sample thickness. Chemical information is carried by the period of these extinction oscillations and different elements can be distinguished. However, at particular sample thicknesses the contrast of columns occupied with different elements can be equal. In the example of figure 3 this is the case for Al, In, and Au columns at ~ 6 nm of sample thickness. Further, extinction oscillations can be exploited

to amplify chemical information as will be shown in section 3. There are significant consequences related to the presence of extinction oscillations. First, the chemical information can be confused at specific sample thicknesses which can only be avoided if thickness gradients are recorded in an image. Second, the interpretability of an image directly relates to sample preparation because traditional ion milling roughens the sample surfaces to typical values of several nm. This is well comparable with an extinction oscillation of heavy elements that is ~ 5 nm short in case of gold. Thus, surface roughness can be confused with chemistry.

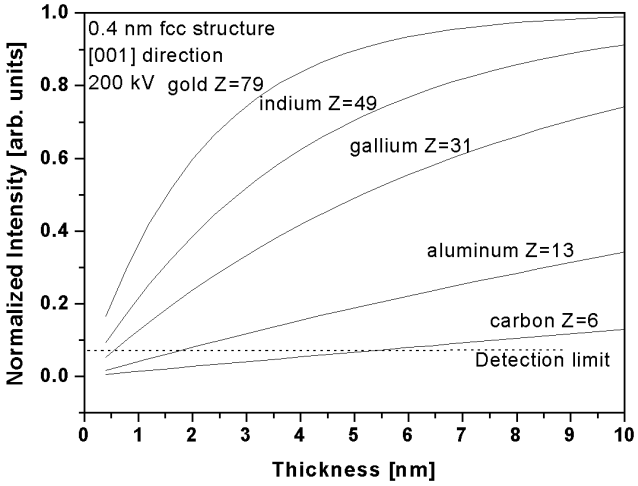

Figure 4: HAADF image intensity versus sample thickness of a fcc crystal with lattice parameter a=0.4 nm and lattice sites occupied by the indicated elements.

The Z - contrast signal, on the other hand, grows exponentially with sample thickness if thin samples are considered. Chemical information is carried by a more rapid signal growth with sample thickness for elements with increasing Z (Figure 4). At a given thickness chemical distinction is unique and the method is less sensitive to changes of sample thickness. Therefore, it is often easier to distinguish different elements by Z-contrast microscopy in particular if they are heavy and noise levels are not limiting.

From a theoretical point of view, there is no doubt that single atoms should be detectable by both techniques. Experimentally, however, the noise level in images, the availability of suitable samples, and their resistance against radiation damage are most limiting factors. It is desirable to characterize microscope performance in terms of the signal to noise ratio for the detection of individual atoms because this value is independent of the applied technique.

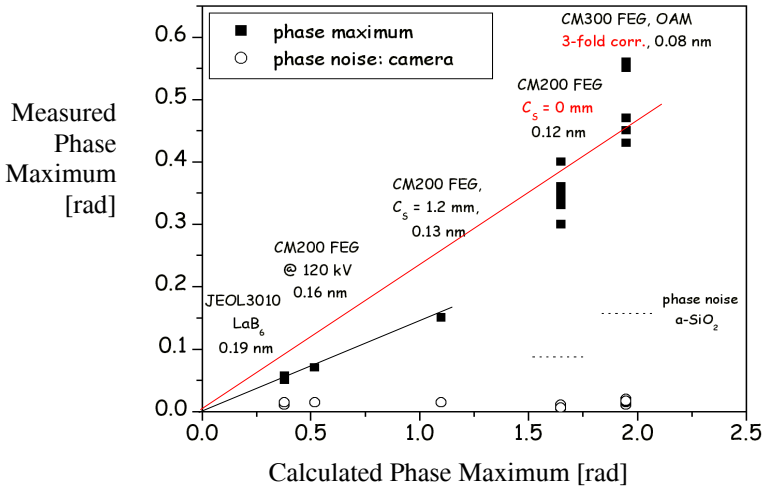

Figure 5: Comparison of microscope performance. Gold [110] crystals are used. Tested microscopes are indicated. For details see text.

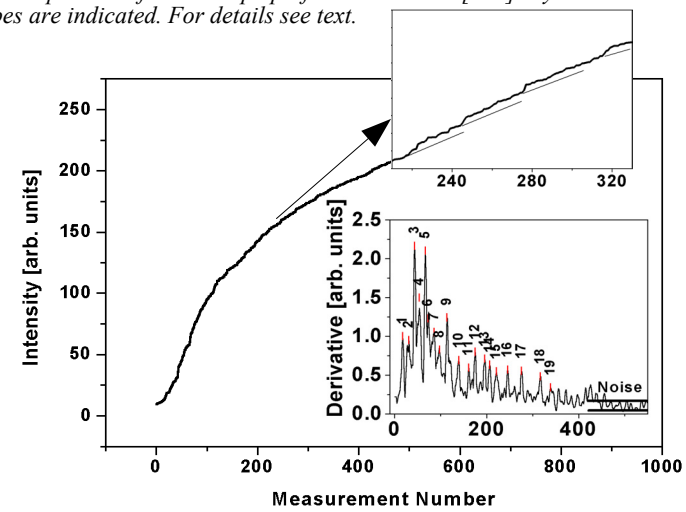

Figure 6: Detection of single gold atoms from Z-contrast images. Intensity maxima are extracted from the HAADF image of figure 2 and sorted accenting (measurement). The curve exhibits discrete jumps (top inset) that can be amplified by taking the derivative of the curve (bottom inset).

Gold is a suitable element for this purpose because of its large electron scattering factor (large Z) and the availability of suitable samples. In order to

achieve this goal, we exploit that phase contrast signals oscillate with sample thickness and, therefore, reach a well defined maximum that can be recovered from a reconstruction of the electron exit wave and compared with expectations [20,21]. Figure 5 sows the result of these experiments. It is seen that phase contrast signals increased by a factor of 10 as a result of resolution improvements that were enabled by replacing the thermionic emitters (LaB_6) with Field Emission Guns (FEG) and by the starting efforts to correct lens aberrations. Phase maxima in gold occur in columns made from 5 gold atoms. Considering the indicated noise levels from CCD cameras one calculates a signal to noise ratio of about 6 for the detection of a single gold atom for the case of the One Ångstrom Microscope in Berkeley. Amorphous layers that are absent from our gold sample but covering many other TEM samples degenerate this S/N ratio substantially (Figure 5).
The signal to noise ratio for the detection of one gold atom from HAADF images can be deduced by identifying experimentally the intensity portion that comes with the addition of a single gold atom to a column [13]. Results are shown in figure 5 that allow estimating a S/N ratio of about 3 for the detection of a single atom by HAADF imaging.

3. Guidelines for the detection of single atoms

An estimate can be given about the detection limit for single atoms from Periodic Table of Elements by phase - and Z-contrast imaging with the current microscope generation utilizing the determined S/N ratios of gold, literature data, and theory. It is given in Figure 7. Phase contrast microscopy generally has a better signal to noise ratio for the detection of single atoms, and one can anticipate that even individual light atoms can be distinguished (Z> 5-10). Z-contrast microscopy allows better discrimination between different elements because of the concave character (amplification) of the signal dependence on Z. Single atom sensitivity is obtained for elements with Z larger than about 40. The discussed thickness dependence of the different types of signal complicates the picture. In addition, the radiation damage caused by 200-300 keV of electron energy, surface roughness, and the presence of amorphous layers currently prevent single atom sensitivity in all but a few cases. These are issues of ongoing research.
Figure 7 can be utilized to understand and design experiments that aim for single atom detection. For example, P. M. Voyles et al. recently reported the detection of single antimony (Z= 51) atoms in silicon (Z=14) by HAADF imaging [14]. From Figure 7 it is seen that single antimony atoms can be detected but single silicon atoms not. On the other hand, silicon samples of 3-4 nm thickness will produce a signal above the detection limit and the addition of a single Sb atom to a silicon column would almost double the signal from the matrix and enable to count antimony atoms in HAADF images as long as their density is small enough such that there are not more than 1 Sb atom in each Si

column. Thus, this experiment could be performed because of the appreciable Z difference of these elements ($\Delta Z = 37$).

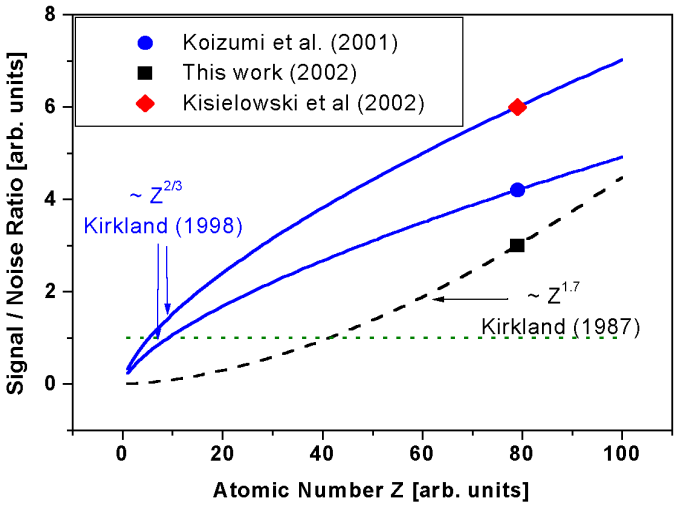

Figure 7: Sensitivity of HRTEM (circle), EWR (diamond), and HAADF imaging (square) for the detection of single atoms with atomic number Z [13]. A signal to noise ratio of 1 is considered to be the detection limit.

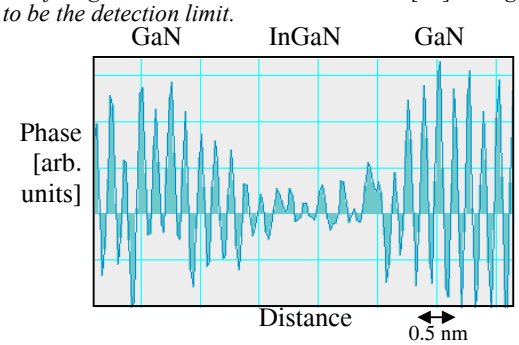

Figure 8: Intensity profile across an GaN/InGaN/GaN quantum well from a reconstructed phase image. The signal reduction in the quantum well is caused by substituting Ga atoms with an average of 2.7 indium atoms in each column.

Phase contrast microscopy does already allow for a detection of columns made from light atoms [8] which remains to be demonstrated for Z-contrast microscopy. One current effort concentrates on the discremination of single indium atoms in a gallium nitride matrix ($\Delta Z = 18$). In Figure 8 an intensity profile across an GaN/InGaN/GaN quantum well from a reconstructed phase image is shown. Here, the faster extinction oscillations of the InGaN compared

with GaN leads to a signal reduction in columns that contain indium. In this sample only 2.7 imdium atoms replace Ga atoms in each column on the average and yet the signal to noise ratio is already suitable to count every indium atoms in each of the columns.

In conclusion, unprecidented technological progress made transmission electron microscopes available with sensitivities that allow already for the detection of single atoms at a resolution that surpassed the one Ångstrom barrier. Currently, such experiments are feasible in selected materials systems. Sample preparation, radiation damage, residual aberrations, and stabilities are limiting factors for a general application of such experiments that can be complemented by spectroscopy on individual columns [12].

4. References

[1] D. Van Dyck, H. Lichte, K.D. van der Mast, Ultramicroscopy 64 (1996) 1
[2] M. Haider, H. Rose, S. Uhlemann, E. Schwan, B. Kabius, K. Urban, Ultramicroscopy 75 (1998) 53
[3] O.L. Krivanek, N. Dellby, A.R. Lupini, Ultramicroscopy 78 (1999) 1
[4] M. Lentzen, B. Jahnen, C. L. Jia, A. Thust, K. Tillmann and K. Urban, Ultramicroscopy 92 (2002) 233
[5] P. E. Batson, N. Dellby & O. L. Krivanek, Nature 418, 617–620 (2002).
[6] E.D. Boyes, J. Rignalda, M.A.J. van der Stam, T.F. Fliervoet, E. Van Cappellen, Microscopy and Microanalysis 7, 2001, 232
[7] P.D. Nellist, S.J. Pennycook, Ultramicroscopy 78 (1999) 111
[8] C. Kisielowski, C.J.D. Hetherington, Y.C. Wang, R. Kilaas, M.A. O'Keefe, A. Thust, Ultramicroscopy 89 (2001) 243
[9] B. Rafferty, S.J. Pennycook, Ultramicroscopy 78 (1999) 141
[10] M.A. O'Keefe, C.J.D. Hetherington, Y.C. Wang, E.C. Nelson, J.H. Turner, C. Kisielowski, J.-O. Malm, R. Mueller, J. Ringnalda, M. Pam, A. Thust, Ultramicroscopy 89 (2001) 215
[11] H. Ohnishi, Y. Kondo, K. Takayanagi, Nature 395 (1998) 780
[12] E.A. Stach, I. Arsian, N. Browning, these proceedings
[13] C. Kisielowski, K. Mitsuishi, J. Rignalda, T. Fliervoet, Sub. PRL (2002)
[14] P. M. Voyles, D. A. Muller, J. L. Grazul, P. H. Citrin,, H.-J. L. Gossmann, Nature 416 (2002) 826
[15] R.F. Klie, Y. Ito, S. Stemmer, N.D. Browning, Ultramicroscopy 86 (2001) 289
[16] W.M.J. Coene, A. Thust, M. Op de Beeck, D. Van Dyck, Ultramicroscopy 64 (1996) 109
[17] A. Thust, W.M.J. Coene, M. Op de Beeck, D. Van Dyck, Ultramicroscopy 64 (1996) 211
[18] D. van Dyck, J.H. Chen, Solid State Communications 109 (1999) 501
[19] S.J. Pennycook, B. Rafferty, P.D. Nellist, Microscopy and Microanalysis 6 (2000) 106
[20] J.R. Jinschek, C. Kisielowski, M. Lentzen, K. Urban, Microscopy and Microanalysis 8 (2002) 466CD
[21] C. Kisielowski, J. Jinschek, K. Mitsuishi, U. Dahmen, M. Lentzen, J. Ringnalda, T. Fliervoet, Proceedings 15th ICEM (2002) 165
[22] R. Kilaas, 45th Ann. Proc. EMSA 1987, 66